European Journal of Chemistry 3 (2) (2012) 191-195

European Journal of Chemistry

Journal homepage: www.eurjchem.com

Photocatalytic degradation of methylene blue using a zinc oxide-cerium oxide catalyst

Venkatesham Vuppala[a], Madhu Gattumane Motappa[a,*], Satyanarayana Suggala Venkata[b] and Preetham Halugondanahalli Sadashivaiah[a]

[a] *Department of Chemical Engineering, M.S. Ramaiah Institute of Technology, Bangalore, 560054, India*
[b] *Department of Chemical Engineering, Jawaharlal Nehru Technological University, Anantapur, 515002, India*

**Corresponding author at: Department of Chemical Engineering, M.S. Ramaiah Institute of Technology, Bangalore, 560054, India. Tel.: +91.080.23606934; fax: +91.080.23603124. E-mail address: madhugm_2000@yahoo.co (M.G. Motappa).*

ARTICLE INFORMATION

Received: 26 November 2011
Received in revised form: 03 February 2012
Accepted: 12 February 2012
Online: 30 June 2012

KEYWORDS

ZnO-Ce_2O_3
Photocatalyst
Nanomaterial
Methylene blue
Gel-combustion
Water treatment

ABSTRACT

The photocatalytic degradation of methylene blue in aqueous solution was studied using a UV source in the presence of zinc oxide-cerium oxide (ZnO-Ce_2O_3) as photocatalyst, which was synthesized by a gel combustion technique and characterized by X-ray diffraction, scanning electron microscopy, and energy dispersive X-ray spectroscopy. The particle size of the catalyst was found to be in between 45 to 60 nm. The effects of catalyst loading (1.0-8.0 g/L), pH (4.0-9.2) and dye concentration (5.0-20.0 mg/L) on the degradation were studied in a batch reactor. The degradation rate was found to be strongly dependent on these experimental parameters. Appreciable degradation of methylene blue was achieved when the catalyst was calcined before use. Best results were observed with a catalyst loading of 5 g/L at pH = 9.2.

1. Introduction

Discharge of industrial dye-containing wastewater is a major source of environmental problems, especially in third world countries [1]. Conventional treatment methods involve either adsorption or chemical coagulation; but these methods only augment the problem since they merely transfer the dyes from the liquid to the solid phase which necessitates further treatment and may result in secondary pollution [2]. Thus, alternative treatment strategies such as semiconductor mediated photocatalytic oxidation can be applied successfully for complete mineralization of organic dyes without causing any secondary pollution.

Use of nanoparticle semiconductors such as titanium dioxide (TiO_2), zinc oxide (ZnO), iron oxide (Fe_2O_3), and cadmium sulphide (CdS) in the photocatalytic degradation of organic pollutants in water and air have attracted attention in the past two decades [1,3-8]. In particular, ZnO nanoparticles have attracted much attention with respect to degradation of many organic pollutants [9, 10]. ZnO is a suitable alternative to TiO_2 (3.2 eV) as it has similar bandgap energy [6], larger quantum efficiency and higher photocatalytic efficiency [3,11-12]. Cerium oxide, a semiconducting material with a bandgap (4.1 eV) [13], has also been considered as a good photocatalyst. Metal oxide coupling can increase the responsiveness of suspended metal oxide particles to the visible and UV light.

The effect of various parameters such as pH and catalyst loading on the degradation of methylene blue (MB) using zinc oxide and zinc oxide doped with other metals were studied by various groups [14-15]. Chakrabarti and Dutta [16] employed zinc oxide catalyst to study the degradation of MB and Eosin Yellow. A maximum degradation of 60% was observed for MB under optimal condition (pH = 9.7, catalyst loading 1.0 g/L, dye concentration of 50.0 mg/L, UV lamp 16 W and air flow rate 6.131/min). The photocatalytic degradation of dye using palladium (Pd) doped ZnO [17] was applied as catalyst for UV-induced degradation of methanol, glucose and sucrose in aqueous solutions in a photocatalytic reactor. ZnO/CdO [18], Mn-doped ZnO [19], thulium ion (Tm^{3+})-doped nanometer ZnO [20] were also used in photocatalytic degradation of MB under visible light. From these reports, it can be concluded that photocatalytic reaction depends on the design, working conditions and the power of UV lamp and the nature of catalyst. In recent years it has been verified that the doping of semiconductors with metals or metallic oxides increases the photocatalytic activity of these semiconductors [21]. Magesh *et al.* studied photocatalytic degradation MB using Ce modified TiO_2 (CeO_2-TiO_2) nanoparticles synthesized by polymer assisted method, which shows that coupling a photocatalyst with high recombination rate to a suitable material will enhance photocatalytic activity [22]. The high UV absorption efficiency leads to the generation of more electrons and holes at the catalyst substrate interface. These electrons and holes are considered the main species involved in the photocatalytic degradation process. The general scheme of the photocatalytic destruction of organic compounds begins with its excitation by suprabandgap photons, and continues through redox reactions where $^{\bullet}OH$ radicals formed on the photocatalyst surface, play a major role in photodegradation [23]. The mechanisms are shown in equations 1-4.

$$ZnO - Ce_2O_3 \rightarrow ZnO - Ce_2O_3\,(h^+ + e) \quad (1)$$

where h^+ = hole and e = electron

$$h^+ + H_2O \rightarrow \cdot OH + H^+ \quad (2)$$

ISSN 2153-2249 (Print) / ISSN 2153-2257 (Online)
DOI:10.5155/eurjchem.3.2.191-195.564

$$h^+ + OH^- \rightarrow \cdot OH \quad (3)$$

$$e + O_2 \rightarrow \cdot O_2^- \quad (4)$$

The objective of the present study involves the preparation, characterization and application of zinc oxide coupled cerium oxide catalyst for the degradation of MB. Synthesis of the catalyst was carried out by self-ignition gel combustion method and its application in photo catalytic degradation of MB dye was explored. The effect of catalyst loading, concentration of the dye and pH on the photo catalytic reaction was studied in detail.

2. Experimental

2.1. Instrumentation

To study the surface morphology and elemental analysis of the photocatalyst, scanning electron microscopy (SEM) and energy dispersive X-ray analysis (EDAX) were carried out (ESEM Quanta 200, FEI, USA). X-ray diffraction study of the catalyst was carried out (Bruker D2 Phaser, USA) at 2θ = 5-60 °, step size of 0.02 ° with a time step 0.5 sec. Methylene blue concentration was estimated using UV-visible (Systronics-117, India) spectrophotometer at wavelength of 663.2 nm. Quartz cuvette of 10 mm path length was used.

2.2. Synthesis of ZnO-Ce_2O_3 and characterization

Synthesis of ZnO-Ce_2O_3 was carried out by gel combustion process. Zinc nitrate hexahydrate (Merck, >96.0%) and cerium (III) nitrate (Himedia, >99.0%) were used with glycine as fuel. Suitable quantities of zinc nitrate, cerium nitrate and glycine were dissolved in 125 mL distilled water, so that the fuel to nitrate molar ratio was maintained as 0.24. The reaction mixture was placed on a hot plate. As the heating progressed, water vapour and nitrates (nitric gases) were released during heating resulting in the formation of gel. The reaction was completed by self-ignition (combustion), minutes after the formation of the gel, leaving behind golden yellow powder. The catalyst was then calcined at 400 °C. The synthesized powder (ZnO-Ce_2O_3) was characterized by SEM, X-ray diffraction (XRD), and (EDAX) to study the surface morphology, size, and composition.

2.3. Evaluation of photocatalytic activity

The reaction set up consisted of a static batch photo reactor of 800 mL capacity, (cylindrical glass flask) open to air. The glass flask was kept on a magnetic stirrer which ensured oxygenation, and uniform mixing of the reaction mixture. Irradiation was assured by artificial light, using two UV lamps of 8 W (Philips), positioned directly above the liquid surface. The distance between the lamp and base of the beaker was 26 cm and the depth of liquid in the beaker was 2.5 cm. Reaction temperature was maintained at ambient conditions (27 ± 3 °C) for all experimental trials. Each experimental run was carried out for 120 min. The concentration of the dye in the reaction mixture was measured at regular interval by measuring the absorbance of the aliquot solution using the UV-visible (Systronics-117) spectrophotometer (at 663.2 nm) with de-ionized water as reference.

3. Results and discussion

3.1. SEM and XRD analysis

Figure 1 shows the SEM pictures of ZnO-Ce_2O_3 particles produced by the gel combustion technique. It shows two different size of particles agglomerated to a certain extent. The small sized spherical particles of cerium oxide were well-dispersed on the pellet type structured zinc oxide. XRD of as-prepared ZnO-Ce_2O_3 is represented in Figure 2a and XRD of 400 °C calcined ZnO-Ce_2O_3 represented in Figure 2b. The peaks in the Figure 2b match with the ZnO and Ce_2O_3 standards. From JCPDS data, Powder Diffraction File. Card no: 89-8435 [24] and Powder Diffraction File. Card no: 36-1451 [25], we can confirm the presence of Ce_2O_3 and ZnO (Wurtzite phase). As-prepared ZnO-Ce_2O_3 XRD shows amorphous morphology and calcined at 400 °C showed crystalline morphology having broad peaks. A crystal size of the sample was calculated by Scherrer's formula (d = 0.94 λ/β cosθ) and was found to be 45-60 nm.

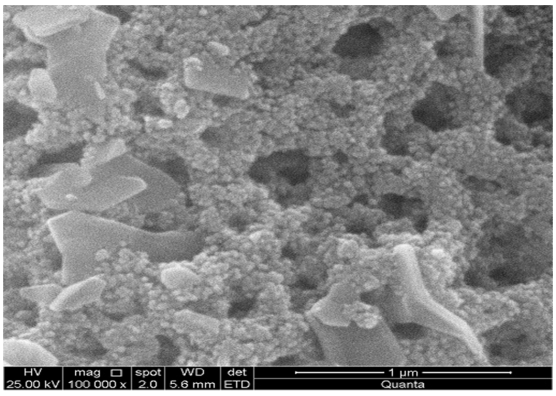

Figure 1. SEM image of ZnO-Ce_2O_3 (magnification 100000X).

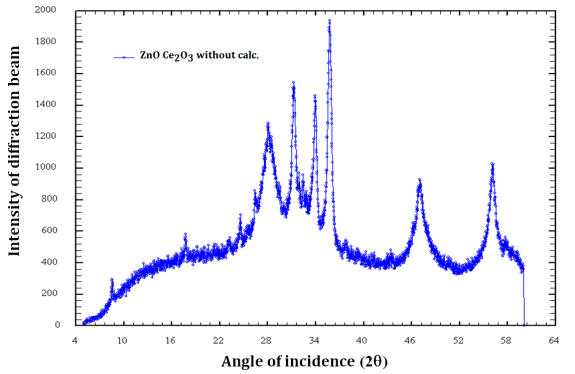

(a)

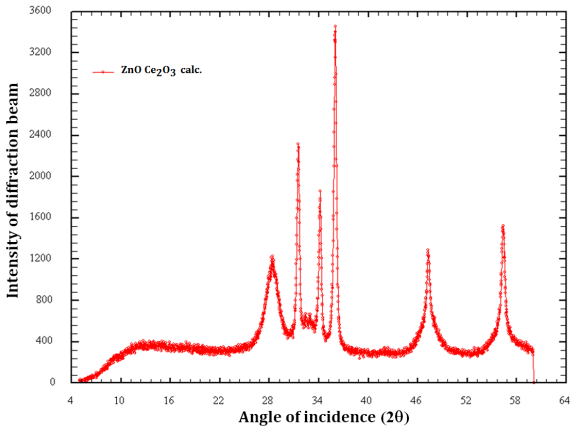

(b)

Figure 2. (a) XRD patterns of ZnO-Ce_2O_3 (without calcined), (b). XRD patterns of calcined (400 °C) ZnO-Ce_2O_3.

3.2. EDAX analysis

EDAX spectrum of ZnO-Ce_2O_3 (Figure 3) shows the peaks for zinc, cerium and oxygen elements indicating that the coupled catalyst is made up of only these elements. Peak indexing of the elements are oxygen 0.525 keV, zinc 8.63 keV, and cerium 5.01 keV. The compositions in mass percentage of the elements are zinc 58.90%, cerium 24.34 %, and oxygen 16.70%. The observed composition matches with the theoretically calculated composition.

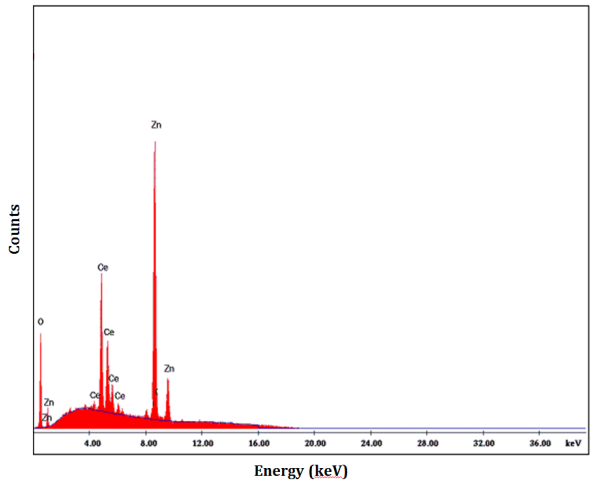

Figure 3. EDAX spectrum of calcined ZnO-Ce_2O_3.

3.3. Photocatalytic activity

3.3.1. Effect of catalyst loading

In order to study the photocatalytic property of the ZnO-Ce_2O_3, experiments were conducted using as-synthesized and calcined catalysts. The effect of the photocatalyst loading, dye concentration and pH on degradation was studied. Pseudo first order kinetic model was used to determine the kinetics of the reaction. To determine the degradation, if any in the absence of the catalyst, test experiment was conducted and it was observed that no degradation occurred. To find the effect of adsorption on solid catalyst, the catalyst was dispersed in the solution and kept in the dark for 60 minutes with stirring, negligible adsorption of the dye was observed.

To determine the optimal amount of the photocatalyst loading, the experiments were carried out by varying catalyst loadings for as-prepared catalyst and calcined catalyst at pH = 7. Initial degradation experiments were conducted using as-prepared (uncalcined) catalyst for catalyst loading (1.0 to 5.0 g/L). The plot of C/C_0 as a function of irradiation time was represented in Figure 4. C is the concentration of dye in the reaction mixture (mg/L) and C_0 is the initial concentration of the dye (mg/L). Maximum degradation of 37% was achieved for catalyst loading of 5.0 g/L for 2 h. From Figure 2a we can observe that XRD of as-prepared ZnO-Ce_2O_3 is amorphous in nature and exhibits very low photocatalytic activity. The amorphous structure leads to the recombination of the photo-generated electrons and holes [26], which in turn reduces the photocatalytic activity. The other possible reason is the presence of trace amounts of nitrate in the catalyst, which may affect the generation of hydroxyl ions which in turn suppress degradation rates.

For calcined ZnO-Ce_2O_3, experiments were conducted using varying catalyst loading of 1.0 to 8.0 g/L. The plot of C/C_0 as a function of irradiation time is represented in Figure 5. It was found that after 2 h, 90% degradation was achieved for catalyst loading of 5.0 g/L at neutral pH. The degradation achieved by calcined ZnO-Ce_2O_3 showed better photocatalytic activity when compared with the uncalcined catalyst. The catalytic degradation MB is better than degradation reported earlier for 10 mg/L dye concentration using different photocatalyst [7,13,23]. The decrease in the rate above 5.0 g/L for calcined catalyst loading is perhaps due to light scattering caused by the suspended catalyst [27-29]. The phenomenon may be explained as follows: with increase in the catalyst loading the incident light penetration to the substrate catalyst interface becomes difficult. Increase in the catalyst concentration may decrease the photoabsorption, which in turn reduces the dye adsorption thus reducing MB degradation. The optimal catalyst loading depends on various factors such as the geometry of the reactor, type of the catalyst, the working condition and incident radiation reflux [27,30-31]. In order to study the degradation kinetics a pseudo first order kinetic model was used .The general rate equation is given as:

$$\frac{-dC}{dt} = k.C.C_{OH^*} \quad (5)$$

where C represents the methylene blue concentration and C_{OH^*} the hydroxyl radical concentration. By the pseudo-stationary hypothesis (i.e. the C_{OH^*} can be considered to be constant because of the continuous hydroxyl ion generation by photocatalysis and the rate depends only on methylene blue concentration), hence the rate expression (5) can be written as (Equation 6)

$$-\ln\left(\frac{C}{C_O}\right) = k.t \quad (6)$$

The linear plot of $\ln\left(\frac{C_O}{C}\right)$ versus t gives the rate constant, k (slope).

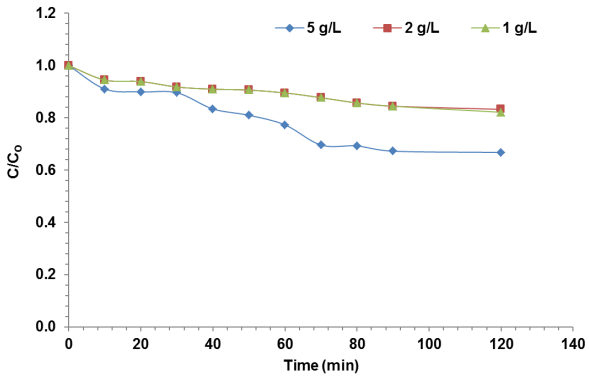

Figure 4. Effect of catalyst loading (without calcined) on the fractional degradation of MB at pH = 7.

The degradation rate data obtained for different catalyst loading were plotted using pseudo first order kinetic model, the fairness of the fit is indicated by the fact that linear regression (r^2) values are greater than 0.9. Therefore the model is in good agreement with the experimental data. The values of the first order rate constant and r^2 are indicated in Table 1.

3.3.2. Effect of concentration

Experiments were conducted to study the effect of dye concentration at constant loading of catalyst 5.0 g/L and pH = 7. The dye concentration was varied from 5.0 to 20 mg/L. An increase in the dye concentration leads to decrease in the rate of its degradation. Plot of C/C_0 versus time is represented in Figure 6.

Table 1. Pseudo-first-order kinetic parameters for degradation of MB at different catalyst loadings (10 mg/L dye concentration, pH = 7).

Catalyst loading (g/L)	k (1/min)	r^2
1	0.008	0.954
2	0.009	0.994
3	0.013	0.972
4	0.013	0.990
5	0.017	0.980
6	0.015	0.997
8	0.016	0.990

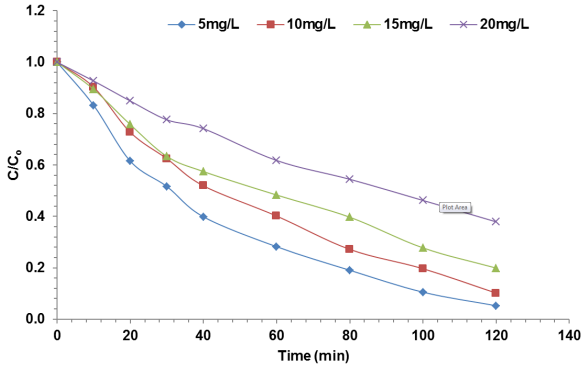

Figure 5. Effect of catalyst loading (calcined) on the photocatalytic degradation of MB at pH = 7.

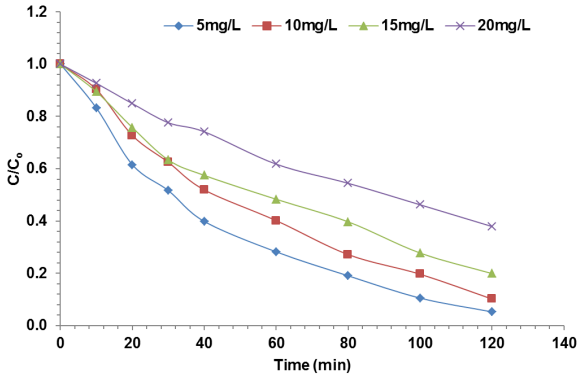

Figure 6. Effect of dye concentration on degradation of MB (5.0 g/L catalyst loading at pH =7).

The degradation rate data obtained for different concentrations of dye was plotted using pseudo-first order kinetic model. The data perfectly fits pseudo-first order kinetics and rate constant data is tabulated in Table 2. k = 0.022 min^{-1} was found to be maximum for dye concentration of 5.0 mg/L. MB degradation decreased as initial concentration increased. A possible reason should be the generation of hydroxyl radicals on the catalyst surface is reduced when the initial MB concentration is increased [32]. More the number of MB molecules adsorbed on the surface of ZnO-Ce_2O_3 photocatalyst will mean fewer active sites are available for the hydroxyl radical adsorption. Once the MB concentration is increased, most of UV light is absorbed by the MB molecules [33], and photons do not reach the surface of photocatalyst to activate it to generate hydroxyl radicals.

Table 2. Pseudo-first-order kinetic parameters for degradation of MB at different initial dye concentration (5.0 g/L catalyst loading, pH = 7).

Concentration (mg/ L)	k (1/min)	r^2
5	0.022	0.988
10	0.017	0.981
15	0.012	0.989
20	0.007	0.997

3.3.3. Effect of pH

The effect of pH on the photocatalytic activity is considered an important parameter as most industrial waste streams are at different pH. In semiconductor mediated photocatalytic reactions, pH is an important parameter because the amphoteric behavior of the semiconducting particles influences the dispersion (suspension) of the catalyst in the substrate. In finely dispersed suspension, the catalytic activity was considered to be very high. To study the pH effect, experiments were carried out at three different pH, acidic (pH = 4), neutral (pH = 7) and basic (pH = 9.2). The MB concentration was maintained constant at 10 mg/L and catalyst loading was maintained at 5.0 g/L. The degradation of MB increased with increase in pH, as presented in Figure 7. The maximum degradation was observed at pH = 9.2. The efficiency at higher pH can be explained on the basis of zero point charge of ZnO-Ce_2O_3.The zero point charge is known as the pH value at which the concentration of protonated and deprotonated surface groups are equal. The zero point charge of zinc oxide is 9 and cerium oxide is around 7 to 9 [13]. When the pH is high, the catalyst surface is negatively charged by adsorbing hydroxyl ions, which favors the formation of hydroxyl radicals. Under acidic medium, the catalyst surface is preferentially covered by dye molecules. Therefore, increase in the pH value generates large hydroxyl ions, which increases the degradation rate. The degradation rate data obtained for different pH were plotted using pseudo first order kinetic model, the rate constants and r^2 values were tabulated in Table 3. k = 0.021 min^{-1} was found to be maximum at pH = 9.2.

Table 3. Pseudo-first-order kinetic parameters for degradation of MB at different pH (10 mg/L dye concentration, 5 g/L catalyst loading).

pH	k (1/min)	r^2
4.0	0.000	0.934
7.0	0.017	0.981
9.2	0.021	0.992

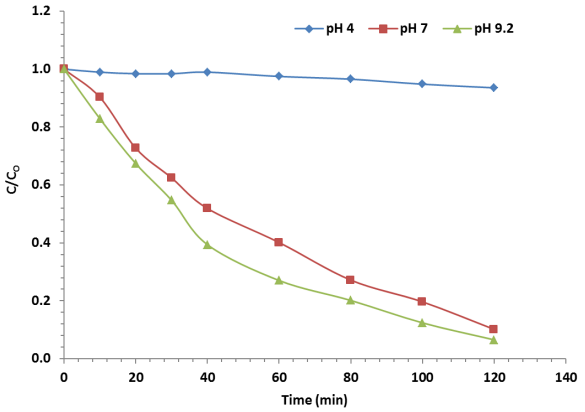

Figure 7. Effect of pH on fractional degradation of MB (10 mg/L dye concentration at 5.0 g/L catalyst loading).

4. Conclusion

Heterogeneous photocatalysis has proved to be very effective in the removal of toxic organic pollutants from the aqueous streams owing its ability to convert them into innocuous products such as carbon dioxide and water. For the first time, an attempt has been made to synthesize ZnO-Ce_2O_3 coupled catalyst by gel combustion technique and its photocatalytic activity explored. Characterization was carried out using SEM, XRD and EDAX. From SEM analysis, it was clearly evident that cerium oxide was coupled (deposited) on zinc oxide.

The EDAX shows the purity of the coupled catalyst and from XRD, we can observe that the particles are crystalline and nano in size. The photocatalytic property of the calcined catalyst was found to be more effective when compared to as-prepared catalyst. The effect of catalyst loading, pH and dye concentration on photocatalytic activity was studied. A maximum degradation of 95% was achieved for a catalyst loading of 5.0 g/L at pH = 9.2. The degradation rate decreased, with increase in dye concentration. A pseudo first order kinetic model was fitted for all the experimental runs and they are in good agreement with the proposed model.

Acknowledgements

The authors thank the Department of Chemical Engineering, M.S. Ramaiah Institute of Technology, Bangalore for providing laboratory facility to carry out research work and also thank Dr Anand Halgeri and Dr Nalini Sundaram, Poornaprajna Institute of Scientific Research, for their guidance and help provided for material characterization.

References

[1]. Matthews, R. W. *Water Res.* **1991**, *25*, 1169-1176.
[2]. Tanaka, K.; Padermpole, K.; Hisanaga, T. *Water Res.* **2000**, *34*, 327-333.
[3]. Sharma, A.; Rao, P.; Mathur, R. P.; Ameta, S. C. *Photochem. Photobio.* **1995**, *86*, 197-200.
[4]. Hong, R. Y.; Li, J. H.; Chen, L. L.; Liu, D. Q.; Li, H. Z.; Zheng, Y.; Ding, J. *Powder Technol.* **2009**, *189*, 426-432.
[5]. Gouvea, C. A. K.; Wypych, F.; Moraes, S. G.; Dura´n, N.; Peralta, Z. P. *Chemosphere* **2000**, *40(4)*, 427-432.
[6]. Sakthivel, S.; Neppolian, B.; Shankar, M. V.; Arabindoo, B.; Palanichamy, M.; Murugesan, V. *Sol. Energ. Mat. Sol. C.* **2003**, *77(1)*, 65-82.
[7]. Madhu, G. M.; Raj, M. A. L. A.; Pai, K. V. K. *J. Environ. Biol.* **2009**, *30(2)*, 259-264.
[8]. Siegel, R. W.; Fujita F. F. (Ed.), Nanophase Materials: Synthesis, Structure, and Properties, Springer Series in Material Science, 27, Springer-Verlag. 1994.
[9]. Sunandan, B.; Jaisai, M.; Imani, R.; Nazhad, M. M.; Dutta, J. *Sci. Technol. Adv. Mat.* **2010**, *11(5)*, 1-7.
[10]. Mansi, C.; Singh, K.; Sandhu, I. S.; Bhatti, H. S. *Nanoscale Res. Let.* **2011**, *6*, 438.
[11]. Gerischer, H.; Heller, A. *J. Phys. Chem.* **1991**, *95*, 5261-5267.
[12]. Cheng, S.; Nickel, U. *Chem. Commun.* **1996**, *2*, 133-134.
[13]. Madhu, G. M.; Raj, M. A. L. A.; Pai, K. V. K.; Rao, S. *Indian J. Chem. Techn.* **2007**, *14*, 139-144.
[14]. Gouvea, C. A. K.; Wypych, F.; Moraes, S. G.; Dura´n, N.; Nagata, N.; Peralta-Zamor, P. *Chemosphere* **2000**, *40(4)*, 433-440.
[15]. Wenzhong, S.; Zhijie, L.; Hui, W.; Yihong, L.; Qingjie, G.; Yuanli, Z**.** *J. Hazard. Mater.* **2008**, *152*, 172-175.
[16]. Chakrabarti, S.; Dutta, B. K. *J. Hazard. Mater.* **2004**, *B112*, 269-278.
[17]. Siriwong, C.; Liewhiran, C.; Wetchakun, N.; Phanichphant, S. Nanoelectronics Conference, 2008. INEC 2008. 2nd IEEE International. "Characterization and photocatalytic activity of Pd-doped ZnO nanoparticles synthesized by flame spray pyrolysis", Chiang Mai Univ., Chiang Mai, Thailand, August 5, 2008, 869-874.
[18]. Saravanan, R.; Shankar, H.; Prakash, T.; Narayanan, V.; Stephen, A. *Mater. Chem. Phys*. **2011**, *125(1-2)*, 277-280.
[19]. Ruh, U.; Dutta, J. *J. Hazard. Mater.* **2008**, *156*, 194-200.
[20]. Jianfeng, W. U.; Feng, L.; Xiaohong, X.; Hao, C.; Zhenggang, R.; Yu, X. *J. Chinese Ceram. Soc.* **2010**, *38(12)*, 2230-2235.
[21]. Alanis-Oaxaca, R.; Jimenez, B. J. *J. Mex. Chem. Soc.* **2010**, *54(3)*, 164-168.
[22]. Ali, R.; Siew, O. B. *J. Teknologi* **2006**, *45(F)*, 31-42.
[23]. Magesh, G.; Viswanathan, B.; Vishwanath, R. P.; Vardarajan, T. K. *Indian J. Chem.* **2009**, *48A*, 480-488.
[24]. Joint Committee on Powder Diffraction Standards, Powder Diffraction File, Card no: 89-8435.
[25]. Joint Committee on Powder Diffraction Standards, Powder Diffraction File, Card no: 36-1451.
[26]. Sakatani, Y.; Grosso, D.; Nicole, L.; Boissiere, C.; Soler, I. G. J. de A. A.; Sanchez, C. *J. Mater. Chem.* **2006**, *16*, 77-82.
[27]. Zhu, C.; Wang, L.; Kong, L.; Yang, X.; Zheng, S.; Chen, F.; Maizhi, F.; Zong, H. *Chemosphere* **2000**, *41*, 303-309.
[28]. Epling, G. A.; Lin, C. *Chemosphere* **2002**, *46*, 561-570.
[29]. Guettai, N.; Ait, A. H. *Desalination* **2005**, 185, 427-437.
[30]. Assabane, A.; Ait Ichou, Y.; Tahiri, H.; Guillard, C.; Hermann, J. M. *Appl. Catal. B-Environ*. **2000**, *24*, 71-87.
[31]. Chen, D.; Ray, A. K. *Appl. Catal. B-Environ.* **1999**, *23*, 143-157.
[32]. Daneshvar, N.; Salari, D.; Niaei, A.; Rasoulifard, M. H.; Khataee, A. R. *J. Environ. Sci. Heal. A* **2005**, *40(8)*, 1605-1617.
[33]. Chung, L. W.; Tan, Y. N.; Mohamed, A. R. *J. Nanotech.* **2011**, 904629, 1-9.